This is an Author's Accepted Manuscript of an article published in Bioprocess and Biosystems Engineering (2012) 35:565-578. The final publication is available at Springer via http://dx.doi.org/10.1007/s00449-011-0629-5

An Optimizing Start-up Strategy for a Bio-methanator*

Mihaela Sbarciog[1], Mia Loccufier[2] and Alain Vande Wouwer[1]

[1]University of Mons, Automatic Control Laboratory, 31 Boulevard Dolez, 7000 Mons, Belgium , Tel.: +32-65374141 , MihaelaIuliana.Sbarciog@Umons.ac.be , Alain.VandeWouwer@Umons.ac.be

[2]Ghent University, Electrical Energy, Systems and Automation, 914 Technologiepark, 9052 Ghent, Belgium, Tel.: +32-92645587 , Mia.Loccufier@UGent.be

Abstract

This paper presents an optimizing start-up strategy for a bio-methanator. The goal of the control strategy is to maximize the outflow rate of methane in anaerobic digestion processes, which can be described by a two-population model. The methodology relies on a thorough analysis of the system dynamics and involves the solution of two optimization problems: steady state optimization for determining the optimal operating point and transient optimization. The latter is a classical optimal control problem, which can be solved using the maximum principle of Pontryagin.

The proposed control law is of the bang-bang type. The process is driven from an initial state to a small neighbourhood of the optimal steady state by switching the manipulated variable (dilution rate) from the minimum to the maximum value at a certain time instant. Then the dilution rate is set to the optimal value and the system settles down in the optimal steady state. This control law ensures the convergence of the system to the optimal steady state and substantially increases its stability region. The region of attraction of the steady state corresponding to maximum production of methane is considerably enlarged. In some cases, which are related to the possibility of selecting the minimum dilution rate below a certain level, the stability region of the optimal steady state equals the interior of the state space. Aside

*This paper presents research results of the Belgian Network DYSCO (Dynamical Systems, Control, and Optimization), funded by the Interuniversity Attraction Poles Programme, initiated by the Belgian State, Science Policy Office. The scientific responsibility rests with its author(s).

its efficiency, which is evaluated not only in terms of biogas production but also from the perspective of treatment of the organic load, the strategy is also characterized by simplicity, being thus appropriate for implementation in real-life systems. Another important advantage is its generality: this technique may be applied to any anaerobic digestion process, for which the acidogenesis and methanogenesis are respectively characterized by Monod and Haldane kinetics.

Keywords— biotechnology, nonlinear systems, stability analysis , optimal control, bang-bang control

1 Introduction

Lately, anaerobic digestion has gained considerable importance, being the most encountered process for the biological treatment of wastewater and biogas production. Compared to the aerobic treatment, the anaerobic digestion provides several advantages among which the higher energy production and the substantially lower sludge production are the most important ones. In terms of process stability, anaerobic digestion still lags behind aerobic biological treatment or physico-chemical processes. Substantial expertise is required to operate such a process properly. From a biological point of view, the main cause of the anaerobic digestion failure is the imbalance between the acid forming bacteria and the methane forming bacteria.

Many control strategies for anaerobic digestion processes have been proposed in the literature, which aim to either regulate the organic pollution level or to optimize the production of the methane gas. The most popular ones are robust output feedback control [1, 2, 3] and adaptive control [4, 5, 6]. In [7], the authors have reviewed a number of control strategies for anaerobic digestion systems and have concluded that neither the classical nor the advanced control methods have succeeded in overcoming all the difficulties which arise in the efficient operation of these processes.

More efficient and less complex control laws may be derived by exploiting the insight gained from a thorough analysis of the system dynamics. This provides useful guidance for process operation and control. The bifurcation and stability analysis of an anaerobic digestion model is presented in [8], where it is concluded that the dynamics of such systems depend heavily on the Haldane-type kinetics describing the growth rate of methanogenic bacteria. This study indicates that a control strategy should be designed so as to trade-off robustness and productivity, which could be quantified by the system stability boundaries. In [9, 10], the authors introduced a risk index for the operation of an anaerobic digestion system, which indicates whether the process has been triggered to a dangerous working

mode. This index was defined based on the areas of the system stability regions and has been recently revisited in [11] based on a rigorous analysis of the nonlinear dynamics.

This paper presents a methodology for the optimization of biogas production in anaerobic digestion systems. Increasing biogas production implies decreasing the organic load in the water, while regulating the organic matter content in the effluent at low values does not necessarily insure high biogas production on a long term. Hence, control strategies which achieve both, a high treatment efficiency and the maximization of the biogas outflow rate, are very attractive from an economical viewpoint. Approaches for multi-objective dynamic optimization of (bio)chemical processes have been reported in [12, 13].

The control strategy developed in this paper has as main goal the optimization of the biogas production during the start-up of a bio-methanator, and it is derived by solving steady state and transient optimization problems. Due to multiple steady states characteristic of these systems, the steady state optimization provides a solution which allows the optimal equilibrium point (characterized by the maximum biogas production) to be reached only from a restricted set of initial conditions. Transient optimization is used to enlarge the set of initial conditions leading the system to the optimum, while insuring maximum biogas production during the transient.

The transient optimization is a classical optimal control problem, which can be solved using the maximum principle of Pontryagin. The procedure is simplified by using one of the system stability boundaries as switching surface, providing thus a suboptimal solution. The resulting control law consists of switching the dilution rate from minimum to maximum and then to the optimal values at well determined time instants. In this way the optimal steady state is reachable from almost the entire state space of the system. Additionally, a high efficiency of the treatment is achieved, as in the optimal steady state approximately 80% of the organic matter is removed. Thus, maximization of biogas production and high treatment efficiency can be simultaneously achieved. Aside its efficiency and simplicity, the method may be applied to any anaerobic digestion process, described by a two-population model, in which the acidogenesis and methanogenesis are respectively characterized by Monod and Haldane kinetics.

2 Process Description

Throughout this paper, an anaerobic digestion model is considered, satisfying the following hypotheses:

- the process takes place in a continuous stirred tank bioreactor;

- two main reactions, acidogenesis and methanogenesis (hydrolysis is not considered a limiting step), describe the process;
- the acidogenesis is characterized by Monod kinetics, the methanogenesis is characterized by Haldane kinetics;
- there is only one feed flow, containing both substrates;
- the concentration of substrates in the influent is constant.

The biological transformations are given by the following reaction network:

$$\begin{aligned} a\xi_1 &\rightarrow c\xi_2 + \xi_3 \\ d\xi_2 &\rightarrow CH_4 + \xi_4 \end{aligned} \tag{1}$$

In the first reaction, the acidogenic bacteria ξ_3 grow on the organic substrate ξ_1 and produce volatile fatty acids ξ_2. In the second reaction, the methanogenic bacteria ξ_4 grow on volatile fatty acids ξ_2 and produce methane. When operating the anaerobic digestion process, a balance between the acidogenesis and methanogenesis must be maintained. Otherwise, the slower growing methanogenic bacteria are washed out and the reactor acidification (accumulation of volatile fatty acids) occurs.

For an ideal continuous stirred tank reactor, the system dynamics described by the reaction network (1) are given by the following differential equations:

$$\dot{\xi}_1 = u(\xi_{in_1} - \xi_1) - ar_1(\xi) \tag{2}$$
$$\dot{\xi}_2 = u(\xi_{in_2} - \xi_2) + cr_1(\xi) - dr_2(\xi) \tag{3}$$
$$\dot{\xi}_3 = -u\xi_3 + r_1(\xi) \tag{4}$$
$$\dot{\xi}_4 = -u\xi_4 + r_2(\xi) \tag{5}$$

while the outflow rate of methane gas reads:

$$Q(\xi) = q\mu_2(\xi_2)\xi_4 \tag{6}$$

In equations (2)-(6), $\xi = \begin{bmatrix} \xi_1 & \xi_2 & \xi_3 & \xi_4 \end{bmatrix}^T \in \mathbb{R}^{+4}$ denotes the state vector. u represents the dilution rate and ξ_{in_1}, ξ_{in_2} respectively represent the concentrations of organic substrate and of volatile fatty acids in the influent. $a, c, d > 0$ are the stoichiometric coefficients. $q > 0$ is the yield for the methane production. The reaction rates $r_1(\xi)$, $r_2(\xi)$ read:

$$r_1(\xi) = \mu_1(\xi_1)\xi_3 \qquad r_2(\xi) = \mu_2(\xi_2)\xi_4 \tag{7}$$

where the growth functions are respectively of Monod and Haldane type

$$\mu_1(\xi_1) = \mu_{m_1}\frac{\xi_1}{K_{s_1}+\xi_1} \tag{8}$$

$$\mu_2(\xi_2) = \mu_{m_2}\frac{\xi_2}{K_{s_2}+\xi_2+\dfrac{\xi_2^2}{K_{i_2}}} \tag{9}$$

Table 1 gives the numerical values/ranges for the anaerobic digestion model parameters and allowable input variables, used for the simulation results.

Table 1: Numerical values/ranges of the anaerobic digestion model parameters and input variables (as in [14])

a	42.14		K_{s_1}	7.1	g/l
c	116.5	mmole/g	K_{s_2}	9.28	mmole/l
d	268	mmole/g	K_{i_2}	256	mmole/l
q	453	mmole/g	ξ_{in_1}	$\begin{bmatrix} 0 & 50 \end{bmatrix}$	g/l
μ_{m_1}	1.2	day^{-1}	ξ_{in_2}	$\begin{bmatrix} 0 & 200 \end{bmatrix}$	mmole/l
μ_{m_2}	0.74	day^{-1}	u	$\begin{bmatrix} 0 & 1.5 \end{bmatrix}$	day^{-1}

By considering a partition of the state vector of the form $\xi = \begin{bmatrix} \xi_a & \xi_b \end{bmatrix}^T$, where $\xi_a = \begin{bmatrix} \xi_3 & \xi_4 \end{bmatrix}^T$ and $\xi_b = \begin{bmatrix} \xi_1 & \xi_2 \end{bmatrix}^T$, and a linear transformation of the states $x_a = \xi_a$, $x_b = \xi_b - C_b C_a^{-1}\xi_a$, a canonical state space representation of the anaerobic digestion system can be obtained [15]:

$$\dot{x}_a = u(w_a - x_a) + C_a\rho(x) \tag{10}$$

$$\dot{x}_b = u(w_b - x_b) \tag{11}$$

with

$$x_a \triangleq \begin{bmatrix} x_3 \\ x_4 \end{bmatrix} \in \mathbb{R}^{+^2};\quad x_b \triangleq \begin{bmatrix} x_1 \\ x_2 \end{bmatrix} \in \mathbb{R}^2;$$

$$C_a = I_2;\quad C_b = \begin{bmatrix} -a & 0 \\ c & -d \end{bmatrix};$$

$$\rho(x) \triangleq \begin{bmatrix} \rho_1(x) \\ \rho_2(x) \end{bmatrix} \in \mathbb{R}^{+^2};$$

$$\rho_i(x) = r_i(\xi)|_{\xi_a = x_a;\ \xi_b = x_b + C_b C_a^{-1} x_a},\ i = 1,2$$

$$w_a = \begin{bmatrix} w_3 \\ w_4 \end{bmatrix} \triangleq \begin{bmatrix} 0 \\ 0 \end{bmatrix};\quad w_b = \begin{bmatrix} w_1 \\ w_2 \end{bmatrix} \triangleq \begin{bmatrix} \xi_{in_1} \\ \xi_{in_2} \end{bmatrix} \in \mathbb{R}^{+^2}$$

The canonical model consists of a nonlinear part of dimension 2 dynamically coupled with a linear part of dimension 2. To preserve the positiveness property of the original system, physical boundary conditions are imposed, which define the state space of the canonical model as:

$$S_x = \{x \in \mathbb{R}^4;\ \xi_1 = x_1 - ax_3 \geq 0; \xi_2 = x_2 + cx_3 - dx_4 \geq 0; \\ \xi_3 = x_3 \geq 0; \xi_4 = x_4 \geq 0\} \tag{12}$$

A detailed analysis of this model has been performed in [16]. For the development of the control strategy, the main properties of the system are summarized here. The anaerobic digestion system (10), (11) has bounded solutions and is a non-oscillatory system. This means that the set of equilibria is globally convergent: as time increases every system solution converges to an equilibrium point. The equilibria are the solutions of

$$x_1 = w_1 = \xi_{in_1} \tag{13}$$
$$x_2 = w_2 = \xi_{in_2} \tag{14}$$
$$[-u + \mu_1(\xi_1)]x_3 = 0 \tag{15}$$
$$[-u + \mu_2(\xi_2)]x_4 = 0 \tag{16}$$

and lie on the plane

$$\Delta = \{x \in S_x;\ x_1 = w_1,\ x_2 = w_2\}$$

The number of physical equilibrium points and their stability properties depend on the magnitude of dilution rate u and of concentrations in the influent of organic substrate ξ_{in_1} and volatile fatty acids ξ_{in_2}.

The equilibrium equations (15), (16) lead to several possibilities:

1. $x_3 = 0$ and $x_4 = 0$

   This defines the equilibrium point A.

2. $x_4 = 0$ and $\mu_1(\xi_1) = u$

   This defines the equilibrium point B, where $\hat{\xi}_{1,B}$ is the unique solution of

   $$\mu_1(\xi_1) = u \tag{17}$$

3. $x_3 = 0$ and $\mu_2(\xi_2) = u$

   This defines the equilibria C and D, generically denoted by M, where $\hat{\xi}_{2,C}$ and $\hat{\xi}_{2,D}$ (with $\hat{\xi}_{2,C} < \hat{\xi}_{2,D}$) are the two solutions of

   $$\mu_2(\xi_2) = u \tag{18}$$

Table 2: The analytical expressions of the system equilibria

Canonical states	Physical states
$\hat{x}_A = \begin{bmatrix} w_1 \\ w_2 \\ 0 \\ 0 \end{bmatrix}$	$\hat{\xi}_A = \begin{bmatrix} \xi_{in_1} \\ \xi_{in_2} \\ 0 \\ 0 \end{bmatrix}$
$\hat{x}_B = \begin{bmatrix} w_1 \\ w_2 \\ \frac{1}{a}(w_1 - \hat{\xi}_{1,B}) \\ 0 \end{bmatrix}$	$\hat{\xi}_B = \begin{bmatrix} \hat{\xi}_{1,B} \\ \xi_{in_2} + \frac{c}{a}(\xi_{in_1} - \hat{\xi}_{1,B}) \\ \frac{1}{a}(\xi_{in_1} - \hat{\xi}_{1,B}) \\ 0 \end{bmatrix}$
$\hat{x}_M = \begin{bmatrix} w_1 \\ w_2 \\ 0 \\ \frac{1}{d}(w_2 - \hat{\xi}_{2,M}) \end{bmatrix}$	$\hat{\xi}_M = \begin{bmatrix} \xi_{in_1} \\ \hat{\xi}_{2,M} \\ 0 \\ \frac{1}{d}(\xi_{in_2} - \hat{\xi}_{2,M}) \end{bmatrix}; M = C,D$
$\hat{x}_N = \begin{bmatrix} w_1 \\ w_2 \\ \frac{1}{a}(w_1 - \hat{\xi}_{1,N}) \\ \hat{x}_{4,N} \end{bmatrix}$	$\hat{\xi}_N = \begin{bmatrix} \hat{\xi}_{1,N} \\ \hat{\xi}_{2,N} \\ \frac{1}{a}(\xi_{in_1} - \hat{\xi}_{1,N}) \\ \hat{\xi}_{4,N} \end{bmatrix}; N = E,F$

$$\hat{x}_{4,N} = \frac{1}{d}\left[w_2 - \hat{\xi}_{2,N} + \frac{c}{a}(w_1 - \hat{\xi}_{1,N})\right] \quad (19)$$

$$\hat{\xi}_{4,N} = \frac{1}{d}\left[\xi_{in_2} - \hat{\xi}_{2,N} + \frac{c}{a}(\xi_{in_1} - \hat{\xi}_{1,N})\right] \quad (20)$$

4. $\mu_1(\xi_1) = u$ and $\mu_2(\xi_2) = u$

   This defines the equilibria E and F, generically denoted by N, where $\hat{\xi}_{1,E} = \hat{\xi}_{1,F}$ is the solution of (17) and $\hat{\xi}_{2,E}$ and $\hat{\xi}_{2,F}$ (with $\hat{\xi}_{2,E} < \hat{\xi}_{2,F}$) are the solutions of (18).

Table 2 presents the analytical expressions of the equilibrium points in the canonical and physical states, respectively, while Fig. 1 presents regions in the spaces $(\xi_{in_1}; u)$, $(\xi_{in_2}; u)$ and $\left(\xi_{in_2} + \frac{c}{a}\xi_{in_1}; u\right)$ corresponding to the occurrence of physical equilibrium points. The first and the second graphs in Fig. 1 are straightforward, as they illustrate the Monod and Haldane character of the reaction kinetics. They respectively express the conditions $\hat{\xi}_{1,B} \leq \xi_{in_1}$ and $\hat{\xi}_{2,M} \leq \xi_{in_2}$ for physical equilibria. The third graph illustrates the condition $\hat{\xi}_{4,N} \geq 0$, which can

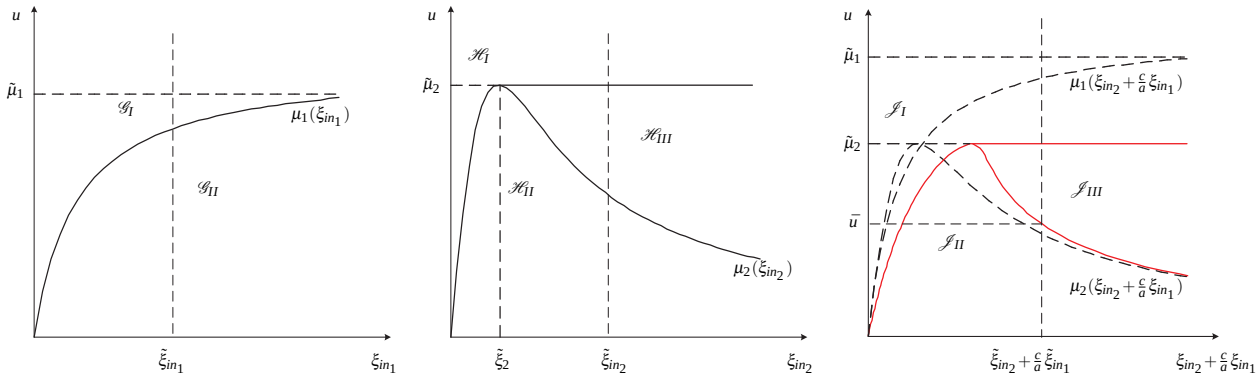

Figure 1: Relationship between the dilution rate u and concentrations of components in the influent ξ_{in_1}, ξ_{in_2} determining a different number of equilibrium points: the regions are bounded by continuous lines. $\tilde{\mu}_1$ and $\tilde{\mu}_2$ respectively represent the limit of the Monod kinetics and the maximum of the Haldane kinetics

be rewritten as $\hat{\xi}_{2,N}+\frac{c}{a}\hat{\xi}_{1,N} \leq \xi_{in_2}+\frac{c}{a}\xi_{in_1}$. The continuous lines show $\hat{\xi}_{2,N}+\frac{c}{a}\hat{\xi}_{1,N}$ as function of $\xi_{in_2}+\frac{c}{a}\xi_{in_1}$. Consequently,

1. $\hat{x}_A$ ($\hat{\xi}_A$), the total wash out of the system, is always a physical equilibrium point;

2. $\hat{x}_B$ ($\hat{\xi}_B$), characterized by the wash out of methanogenic bacteria, is physical if $(\xi_{in_1}, u) \in \mathscr{G}_{II}$;

3. $\hat{x}_M$ ($\hat{\xi}_M$), characterized by acidogenic bacteria wash out, are respectively physical if $(\xi_{in_2}, u) \in \mathscr{H}_{II} \cup \mathscr{H}_{III}$ for $M = C$ and $(\xi_{in_2}, u) \in \mathscr{H}_{III}$ for $M = D$;

4. $\hat{x}_N$ ($\hat{\xi}_N$), characterized by the coexistence of the bacteria populations involved in a syntrophic relationship, are physical if $(\xi_{in_1}, u) \in \mathscr{G}_{II}$ and, for $N = E$, $\left(\xi_{in_2}+\frac{c}{a}\xi_{in_1}, u\right) \in \mathscr{J}_{II} \cup \mathscr{J}_{III}$, while for $N = F$, $\left(\xi_{in_2}+\frac{c}{a}\xi_{in_1}, u\right) \in \mathscr{J}_{III}$. These two equilibria are the operating points of interest. Note that these equilibria are physical only if the acidification point $\hat{x}_B$ is physical.

The stability of equilibria has been assessed via the linearization principle (see [16]). The following characteristics are useful for further development of the control strategy:

- $\hat{x}_E$ is always locally asymptotically stable;
- $\hat{x}_F$ is always unstable;
- $\hat{x}_B$ is locally asymptotically stable in the region where $\hat{x}_F$ is physical (i.e. $\mathscr{J}_{III}$) and unstable in the region where $\hat{x}_F$ is not physical (i.e. $\mathscr{J}_{II}$).

Usually in practice only the dilution rate u can be manipulated, therefore in what follows the inlet concentrations ξ_{in_1} and ξ_{in_2} are considered fixed and set respectively to the values $\tilde{\xi}_{in_1} = 40$ g/l and $\tilde{\xi}_{in_2} = 175$ mmol/l for the simulation results.

3 Optimization

The control purpose is to optimize the methane outflow rate (6) by manipulating the dilution rate u, which is constrained to lie in the interval $[u_{min}, u_{max}]$. The numerical values of u_{min} and u_{max} are selected based on a number of considerations discussed in the next section. During the transient an optimal production of biogas is pursued, possibly taking some costs into account (e.g. minimize the work of the actuator). At the end of the transient period the process should reach a steady state in which the outflow rate of biogas is maximum. Hence the control strategy proposed in this section performs transient as well as steady state optimization.

3.1 Steady state optimization

The steady state optimization problem is defined as follows: *Find the optimal setpoint* $\hat{x}_s = \hat{x}_E^{u_s}$ *(*$\hat{\xi}_s = \hat{\xi}_E^{u_s}$*) and the corresponding optimal dilution rate* $u_s \in [u_{min}, u_{max}]$ *for which the outflow rate of methane* $Q(\hat{\xi}_s)$ *is maximum.*

The analysis summarized in the previous section shows that the only technologically meaningful equilibrium points are $\hat{x}_E$ and $\hat{x}_F$. Both are characterized by methane production. It is easy to see however, that the flow rate of methane produced in $\hat{\xi}_E$ is higher than the flow rate of methane produced in $\hat{\xi}_F$ ($\mu_2(\hat{\xi}_{2,E}) = \mu_2(\hat{\xi}_{2,F}) = u$ and according to (20), $\hat{\xi}_{4,E} > \hat{\xi}_{4,F}$ because $\hat{\xi}_{2,E} = \hat{\xi}_{2,C} < \hat{\xi}_{2,F} = \hat{\xi}_{2,D}$). Consequently, the optimal setpoint is an equilibrium point of type E. Thus, in the optimal equilibrium point $\hat{\xi}_s$ the flow rate of methane is given by

$$Q(\hat{\xi}_s) = q\mu_2(\hat{\xi}_{2,s})\frac{1}{d}\left[\xi_{in_2} - \hat{\xi}_{2,s} + \frac{c}{a}(\xi_{in_1} - \hat{\xi}_{1,s})\right] \tag{21}$$

Calculating $\dfrac{dQ}{d\hat{\xi}_{2,s}} = 0$ leads to

$$\left[\xi_{in_2} - \hat{\xi}_{2,s} + \frac{c}{a}(\xi_{in_1} - \hat{\xi}_{1,s})\right] \cdot \mu_2'(\hat{\xi}_{2,s}) - \mu_2(\hat{\xi}_{2,s})\left(1 + \frac{c}{a}\left.\frac{d\xi_1}{d\xi_2}\right|_{\xi_2 = \hat{\xi}_{2,s}}\right) = 0 \tag{22}$$

where $\left.\frac{d\xi_1}{d\xi_2}\right|_{\xi_2=\hat{\xi}_{2,s}}$ results from

$$\mu_1'(\hat{\xi}_{1,s}) \left.\frac{d\xi_1}{d\xi_2}\right|_{\xi_2=\hat{\xi}_{2,s}} = \mu_2'(\hat{\xi}_{2,s}) \tag{23}$$

with μ_2' denoting the derivative of μ_2 w.r.t. ξ_2 and μ_1' denoting the derivative of μ_1 w.r.t. ξ_1.

Recall that the optimal setpoint is a type E equilibrium point where

$$\mu_1(\hat{\xi}_{1,s}) = \mu_2(\hat{\xi}_{2,s}) = u_s \tag{24}$$

Then (22) and (24) provide sufficient conditions to fully determine the optimal equilibrium point $\hat{\xi}_s$ and the optimal dilution rate u_s.

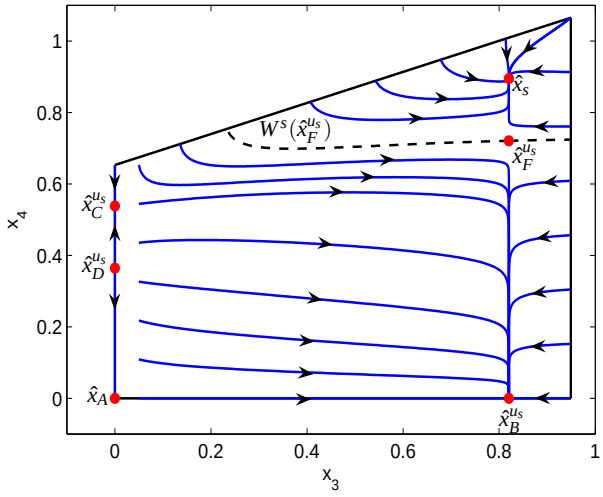

Figure 2: The phase portrait on the Δ plane of the system operated with the dilution rate u_s

Fig. 2 presents the phase portrait on the Δ plane of the system operated with the optimal dilution rate u_s (the superscript in the notation of equilibria indicates the dilution rate). The optimal setpoint $\hat{x}_s$ may be reached only if the initial state of the system lies in its region of attraction, which is defined as

$$\Omega(\hat{x}_s) = \{x_0 \in S_x;\ x(t,x_0) \to \hat{x}_s \text{ for } t \to +\infty\} \tag{25}$$

i.e. the set of initial states from which the steady state $\hat{x}_s$ may be reached.

$\Omega(\hat{x}_s)$ and $\Omega(\hat{x}_B^{u_s})$ (i.e. the attraction region of the acidification point $\hat{x}_B^{u_s}$) are separated by the stability boundary [17]

$$\partial\Omega(\hat{x}_s) = \partial\Omega(\hat{x}_B^{u_s}) = W^s(\hat{x}_F^{u_s}) \tag{26}$$

where $W^s(\hat{x}_F^{u_s})$ (represented with a dashed line in Fig. 2) denotes the stable manifold of the unstable equilibrium point $\hat{x}_F^{u_s}$, which is defined as:

$$W^s(\hat{x}_F^{u_s}) = \left\{x_0 \in S_x;\ x(t,x_0) \to \hat{x}_F^{u_s} \text{ for } t \to +\infty\right\} \tag{27}$$

Thus, $W^s(\hat{x}_F^{u_s})$ represents the set of initial states from which the system converges to the equilibrium point $\hat{x}_F^{u_s}$. Any initial condition lying above $W^s(\hat{x}_F^{u_s})$ leads the system to the optimal steady state $\hat{x}_s$, while any initial state lying below $W^s(\hat{x}_F^{u_s})$ leads the system to the undesired acidification point $\hat{x}_B^{u_s}$. Note that the optimal steady state can be reached only if initially a high concentration of methanogenic bacteria is present in the reactor.

3.2 Transient optimization

The transient optimization problem is formulated as a free final time optimal control problem of the form: *Find the dilution rate* $u(t) \in [u_{min}, u_{max}]$ *which drives, in finite time, the system* (10), (11) *from an initial state at time* $t = 0$ *to a small neighbourhood* S *of the steady state optimal equilibrium point* $\hat{x}_s$*, while minimizing a cost index of the form*

$$J(u) = \int_0^{t_f} [\alpha_1 u - Q]\, dt = \int_0^{t_f} [\alpha_1 u - q\mu_2(\xi_2)\xi_4]\, dt \tag{28}$$

where t_f represents the final time of the control interval and α_1 is a weighting coefficient. In (28), the first term stands for the minimization of the pump work during the transient or minimization of the total culture volume sent through the reactor in non-optimal conditions, while the second term stands for the maximization of the biogas outflow rate and implicitly for the maximization of the methanogenic bacteria growth [18].

As soon as the system state reaches the neighbourhood S (target set) the control effort is switched to $u = u_s$, which ensures the convergence to the optimal steady state for $t \to +\infty$. The boundary of the target set S is generically defined as

$$\partial S = \{x \in S_x;\ \theta(x) = 0\} \tag{29}$$

where $\theta(x)$ is a function of system states. Indications regarding its choice are given below.

The transient optimization is a classical optimal control problem, which can be solved using Pontryagin's maximum principle. Consequently, minimizing the cost index (28) is equivalent to maximizing the Hamiltonian

$$\begin{aligned} H = {} & [\alpha_1 u - q\mu_2(\xi_2)x_4] + p_1 u\,(w_1 - x_1) + p_2 u\,(w_2 - x_2) + \\ & p_3\,[u(w_3 - x_3) + \mu_1(\xi_1)x_3] + p_4\,[u(w_4 - x_4) + \mu_2(\xi_2)x_4] \end{aligned} \tag{30}$$

$p = \begin{bmatrix} p_1 & p_2 & p_3 & p_4 \end{bmatrix}^T$ is the costate vector, where

$$\dot{p}_1 = -\frac{\partial H}{\partial x_1} = p_1 u - p_3 x_3 \mu_1'(\xi_1) \tag{31}$$

$$\dot{p}_2 = -\frac{\partial H}{\partial x_2} = p_2 u + (q - p_4) x_4 \mu_2'(\xi_2) \tag{32}$$

$$\dot{p}_3 = -\frac{\partial H}{\partial x_3} = p_3[u - \mu_1(\xi_1) + a x_3 \mu_1'(\xi_1)] + c(q - p_4) x_4 \mu_2'(\xi_2) \tag{33}$$

$$\dot{p}_4 = -\frac{\partial H}{\partial x_4} = p_4 u + (q - p_4)[\mu_2(\xi_2) - d x_4 \mu_2'(\xi_2)] \tag{34}$$

The transversality conditions at the final time read

$$\left[\left(\frac{\partial \theta}{\partial x} \right)^T \lambda - p \right]_{t=t_f} = 0 \tag{35}$$

where λ are Lagrange multipliers.

The Hamiltonian is linear in the control input and therefore can be written as

$$H \stackrel{\Delta}{=} s_1(x,p)u + s_2(x,p) \tag{36}$$

where

$$s_1(x,p) = \alpha_1 + \sum_{i=1}^{4} p_i (w_i - x_i) \tag{37}$$

$$s_2(x,p) = p_3 \mu_1(\xi_1) x_3 + (p_4 - q) \mu_2(\xi_2) x_4 \tag{38}$$

Notice that:

- the system dynamics are stationary;
- the final time t_f is free;
- the cost index does not contain a term in the final conditions;
- the target set S does not depend on time.

Under these conditions, along an optimal trajectory

$$H = s_1(x,p)u + s_2(x,p) \equiv 0, \qquad 0 \le t \le t_f \tag{39}$$

Hence by the maximum principle, if in an interval (t_1, t_2):

$$s_1(x,p) > 0 \quad \Rightarrow \quad u(t) = u_{min} \quad \text{for } t_1 < t < t_2 \tag{40}$$

$$s_1(x,p) < 0 \quad \Rightarrow \quad u(t) = u_{max} \quad \text{for } t_1 < t < t_2 \tag{41}$$

$$s_1(x,p) = 0 \quad \Rightarrow \quad (t_1, t_2) \text{ is a singular interval} \tag{42}$$

In the case of a singular interval, Pontryagin's maximum principle does not provide any information on the control input u, which has to be computed using other methods. However, it can be shown that for the system (10), (11), singular intervals cannot occur. The proof is included in the appendix. Thus, it may be concluded that:

- the optimal control strategy is of the bang-bang type;
- in the state space of system (10), (11) there exists a switching surface $s_1(x) = 0$ such that for $x \notin S$:

$$s_1(x) > 0 \Rightarrow u = u_{min}$$

$$s_1(x) < 0 \Rightarrow u = u_{max}$$

- for $x \in S$, $u = u_s$.

The switching surface $s_1(x) = 0$ depends on the choice of the target set S and on the weighting parameter α_1 in the cost index. Its determination requires the solution of a set of nonlinear canonical differential equations (10), (11), (31)- (34) with split boundary conditions (initial conditions at $t = 0$, final conditions and transversality conditions at $t = t_f$), which generally constitute a difficult numerical problem (see [19] and references therein). In order to avoid this issue the switching is chosen to take place on a heuristically selected switching surface, leading thus to a suboptimal but simple solution. However, this is also a delicate problem, as the switching surface must satisfy several conditions that have to be checked by simulation:

- The switching surface must be selected such that chattering along this surface is avoided. High frequency switchings in the control input are undesirable as they cause stress on the actuators that might lead to permanent damage.
- The target set must include the operating point $\hat{x}_E^{u_{max}}$. Otherwise the system may settle down in $\hat{x}_E^{u_{max}}$, situation when the switch from u_{max} to u_s in the final stage of the control interval does not occur. Then, the optimal steady state $\hat{x}_s$ is not reached.

- The switching surface must lie in the region of attraction $\Omega(\hat{x}_E^{u_{max}})$ to ensure the system convergence to the target set S after switching from u_{min} to u_{max}. Otherwise the system is driven to the acidification point $\hat{x}_B^{u_{max}}$, where methanogenic bacteria are washed out, precluding thus biogas formation and favoring volatile fatty acids accumulation.

To avoid the tremendous simulation work [20] involved in checking the conditions on the switching surface for all possible initial states of the system, here it is proposed to switch the dilution rate from minimum (u_{min}) to maximum (u_{max}) once the system trajectory reaches the stability boundary $\partial\Omega(\hat{x}_E^{u_{max}}) = W^s(\hat{x}_F^{u_{max}})$. Since the stability boundary is a system trajectory, high frequency switchings cannot occur. Moreover, $\partial\Omega(\hat{x}_E^{u_{max}})$ lies in $\Omega(\hat{x}_E^{u_{max}})$, if it is properly estimated.

An accurate estimation of the stability boundary can be obtained using a trajectory reversing algorithm [21]. A detailed discussion of determining the stability boundary for the anaerobic digestion model (10), (11) can be found in [22]. A simple choice for the target set S is an ellipsoid or ball with the center at the optimal setpoint $\hat{x}_s$ and radius such that $\hat{x}_E^{u_{max}}$ lies inside the target set.

4 Discussion and simulation results

The control strategy described in the previous section indicates that the system must be operated with the dilution rate u_{min} until the switching surface $W^s(\hat{x}_F^{u_{max}})$ is reached. Then, $u = u_{max}$ and the system is operated with the new dilution rate until it enters the target set S. Once inside the target set, the dilution rate is switched to the optimal dilution rate u_s and the system will settle down in the optimal equilibrium point $\hat{x}_s$.

To apply this control strategy, the following steps need to be performed:

- Determine the optimal steady state. To this end, relationships (22), (24) must be used to compute $\hat{x}_s$ and u_s;

- Choose u_{min} and u_{max}, the minimum respectively maximum dilution rates the system can be operated with. These may be imposed either by the physical limitations on the actuator or may be chosen according to the constraints and implications discussed below;

- Compute $\hat{x}_E^{u_{max}}$ and choose the target set S such that $\hat{x}_E^{u_{max}}$ lies in S. Here, a target set with the boundary

$$\theta(x) = \sum_{i=1}^{i=4} \frac{(x_i - \hat{x}_{i,s})^2}{x_{i,r}^2} = 1$$

has been used, where $x_{i,r}$ have been freely selected such that the condition $\hat{x}_E^{u_{max}} \in S$ holds;

- Estimate the stability boundary $W^s(\hat{x}_F^{u_{max}})$.

For the parameter values given in Table 1 and $\xi_{in_1} = \tilde{\xi}_{in_1}$, $\xi_{in_2} = \tilde{\xi}_{in_2}$, steady state optimization leads to the optimal dilution rate $u_s = 0.5179$ day^{-1} and the corresponding optimal equilibrium point

$$\begin{aligned} \hat{x}_s &= \begin{bmatrix} 40 & 175 & 0.82 & 0.9 \end{bmatrix}^T \\ \hat{\xi}_s &= \begin{bmatrix} 5.39 & 29.65 & 0.82 & 0.9 \end{bmatrix}^T \end{aligned}$$

This means that the system inputs are such that $(\xi_{in_1}, u_s) \in \mathscr{G}_{II}$, $(\xi_{in_2}, u_s) \in \mathscr{H}_{III}$, $\left(\xi_{in_2} + \frac{c}{a}\xi_{in_1}, u_s\right) \in \mathscr{J}_{III}$, case in which all six equilibria are physical. The boundary of the target set on the plane Δ is

$$\theta(x_3, x_4) = (x_3 - x_{3,s})^2 / r_x^2 + (x_4 - x_{4,s})^2 / r_y^2 - 1 = 0 \tag{43}$$

with $r_x = 0.015$, $r_y = 0.07$ such that $\hat{x}_E^{u_{max}}$ lies inside S.

While u_s is the solution of the steady state optimization problem, the minimum and maximum dilution rates u_{min} and u_{max} must be selected according to the system characteristics and technological considerations. Below, the selection of u_{min} and u_{max} based on the system characteristics is presented first. Then the impact of several technological issues on the system productivity is briefly discussed. Consequently, the maximum dilution rate $u_{max} > u_s$ must be chosen such that $\hat{x}_E^{u_{max}}$ and $\hat{x}_F^{u_{max}}$ are physical equilibrium points, which means that $u_{max} < \tilde{\mu}_2$ (see Fig. 1). Values of u_{max} higher than $\tilde{\mu}_2 = \frac{\mu_{m_2}}{1+2\sqrt{\frac{K_{S_2}}{K_{I_2}}}}$ correspond to situations in which there is no production of biogas as either the total wash out or the methanogens wash out occurs. Here, $u_{max} = 0.535$ day^{-1} ($\tilde{\mu}_2 = 0.536$) and the same situation as for u_s, characterized by the maximum number of physical equilibrium points, is obtained.

With regard to the minimum dilution rate $u_{min} < u_s$, two alternatives may be possible: $u_{min} \geq \bar{u}$ and $u_{min} < \bar{u}$ (see Fig. 1). $\bar{u}$ is the dilution rate for which $\hat{\xi}_{2,N} + \frac{c}{a}\hat{\xi}_{1,N} = \tilde{\xi}_{in_2} + \frac{c}{a}\tilde{\xi}_{in_1}$ and can be computed from (17) and (18). For the parameter values given in Table 1 $\bar{u} = 0.3495$ day^{-1}. Simulation results are presented below for both situations:

1. $u_{min} \geq \bar{u}$

   This case corresponds to $(\xi_{in_1}, u_{min}) \in \mathscr{G}_{II}$, $(\xi_{in_2}, u_{min}) \in \mathscr{H}_{III}$ and $\left(\xi_{in_2} + \frac{c}{a}\xi_{in_1}, u_{min}\right) \in \mathscr{J}_{III}$ (see Fig. 1), hence both $\hat{x}_E^{u_{min}}$ and $\hat{x}_F^{u_{min}}$ are physical equilibrium points.

Thus the number of equilibria of the controlled system does not change with switching the dilution rate. Fig. 3 shows the phase portrait on the Δ plane of the controlled system. The minimum dilution rate has been chosen as $u_{min} = 0.38$ day^{-1}. Equilibria of the system operated with the dilution rate u_{min} are represented with triangles, those corresponding to u_{max} with squares and those corresponding to u_s are represented with circles. The system stability boundaries $W^s(\hat{x}_F^{u_{min}})$ and $W^s(\hat{x}_F^{u_{max}})$ are represented with dashed lines. The physical state space on the Δ plane is defined by physical boundaries, which are illustrated with continuous lines. The initial condi-

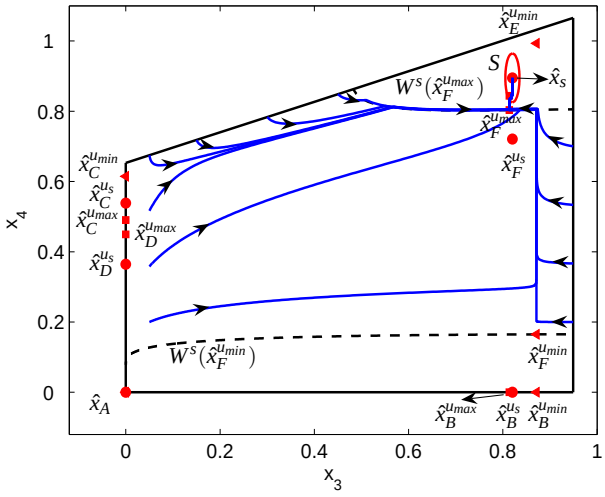

Figure 3: The phase portrait on the Δ plane of the controlled system (case 1)

tion of the system may be selected among the states lying above $W^s(\hat{x}_F^{u_{min}})$. The system is operated with u_{min} until the trajectory reaches the switching surface $W^s(\hat{x}_F^{u_{max}})$, then the dilution rate is switched to u_{max}. The system trajectory moves along the stability boundary $W^s(\hat{x}_F^{u_{max}})$ and, as time increases, will converge to the target set S. When the target set is reached, the dilution rate is set to u_s and the system will settle down in the optimal equilibrium point.

It is worth to notice the enlargement of the attraction region of the optimal equilibrium point compared to the one shown in Fig. 2: now any system trajectory starting in an initial state lying above $W^s(\hat{x}_F^{u_{min}})$ reaches the optimal setpoint $\hat{x}_s$. Hence, $\Omega(\hat{x}_s)$ of the controlled system equals the attraction region of $\hat{x}_E^{u_{min}}$. Notice that in this situation the reactor acidification may still occur due to an inadequate choice of initial condition: if initially the concentration of methanogens is very low, the system will settle down in the acidification point $\hat{x}_B^{u_{min}}$.

2. $u_{min} < \bar{u}$

   Now the system inputs are such that $(\xi_{in_1}, u_{min}) \in \mathscr{G}_{II}$, $(\xi_{in_2}, u_{min}) \in \mathscr{H}_{II}$ and $\left(\xi_{in_2} + \frac{c}{a}\xi_{in_1}, u_{min}\right) \in \mathscr{J}_{II}$, where the system possesses four physical equilibria: $\hat{x}_A^{u_{min}}$, $\hat{x}_B^{u_{min}}$, $\hat{x}_C^{u_{min}}$, $\hat{x}_E^{u_{min}}$. Only $\hat{x}_E^{u_{min}}$ is locally asymptotically stable. Thus, every trajectory starting in an initial state characterized by the presence in the reactor of both bacteria type ($x_3(0) > 0, x_4(0) > 0$) will converge to it.

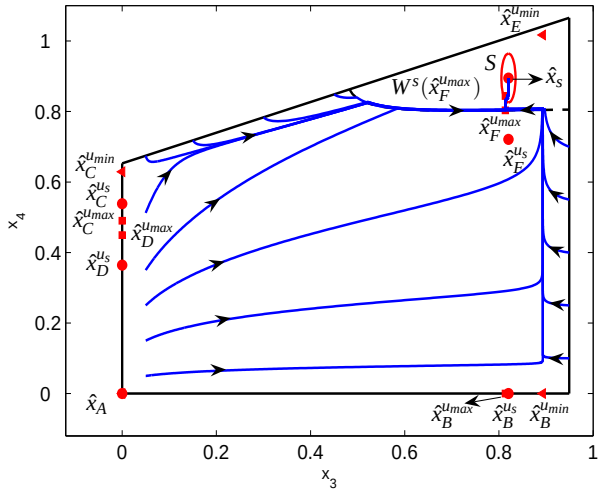

Figure 4: The phase portrait on the Δ plane of the controlled system (case 2)

The change in the structure of the phase portrait does not impose additional constraints on the magnitude of u_{min}. As in the previous case, in order to be able to switch the dilution rate when the system trajectory hits the stability boundary $W^s(\hat{x}_F^{u_{max}})$, $\hat{x}_E^{u_{min}}$ must lie in $\Omega(\hat{x}_E^{u_{max}})$. Otherwise, the system settles down in $\hat{x}_E^{u_{min}}$ and the optimal setpoint will not be reached. It may be checked however, that irrespective of the choice of u_{min}, $\hat{x}_E^{u_{min}}$ lies above $W^s(\hat{x}_F^{u_{max}})$. This is easy to show using the analytical expressions of the equilibria in Table 2, since all equilibria lie on the Δ plane.

Fig. 4 shows the phase portrait on the Δ plane of the controlled system, corresponding to this case. The minimum dilution rate has been chosen as $u_{min} = 0.3$ day^{-1} and the same notations as in Fig. 3 have been used. The optimal equilibrium point $\hat{x}_s$ can be reached now from any initial state characterized by the presence in the reactor of both bacteria type. Hence, in the controlled system $\hat{x}_s$ is quasi-globally asymptotically stable.

As shown above, in the controlled case, the magnitude of u_{min} influences the size of the attraction region of the optimal equilibrium point and will certainly

have an impact on the transient productivity and the time needed to reach the target set. If technologically possible, one would select $u_{min} < \bar{u}$ to take advantage of the fact that the operation can be started in any initial condition in the interior of the state space, i.e. in any initial state with $x_3(0) > 0$ and $x_4(0) > 0$. This is similar to the usual procedure of starting-up anaerobic digesters, when the system is operated with a low dilution rate in order to avoid biomass wash out [23]. If u_{min} cannot be selected smaller than $\bar{u}$, then the second best choice is the closest value to $\bar{u}$, which can be allowed. This will correspond to the widest possible region of attraction of the optimal steady state, however it will still require the verification of the condition $x(0) \in \Omega(\hat{x}_E^{u_{min}})$ such that reactor acidification in the first stage of the control is avoided.

Fig. 5 presents the time evolution of organic substrate, volatile fatty acids, acidogens and methanogens for three controlled situations. In each operation, the initial condition is the same, but a different value for u_{min} is assumed. The control laws, the corresponding methane gas flows produced during each operation as well as the purity of the effluent - expressed as total consumed COD (chemical oxygen demand) - are shown. Noticeably in these simulations is the fact that the transient period (t_f - the time needed to reach the target set) increases with u_{min}. The transient times and the evaluation of the cost index for the considered u_{min} values are given in Table 3. Based on these simulation results, one may conclude

Table 3: The transient period and the cost index evaluation for several choices of u_{min}

u_{min}	t_f	J
0.38	61.43	-9761.89
0.3	47.99	-8748.39
0.1	43.39	-8354.46

that choosing a lower u_{min} not only increases the size of the attraction region of the optimal setpoint but also decreases the transient time. However, further investigations are needed for various initial conditions, which will be detailed in a forthcoming paper.

The water treatment efficiency is evaluated as the decrease in the total COD (chemical oxygen demand). Normally, a decrease of $50-60\%$ is expected for an anaerobic digestion process. To further increase the treatment, the anaerobic process is usually connected with an aerobic process [24].

The COD entering the reactor (COD_{in}) is given by:

$$COD_{in}(g/l) = \xi_{in_1} + 0.6\xi_{in_2} \tag{44}$$

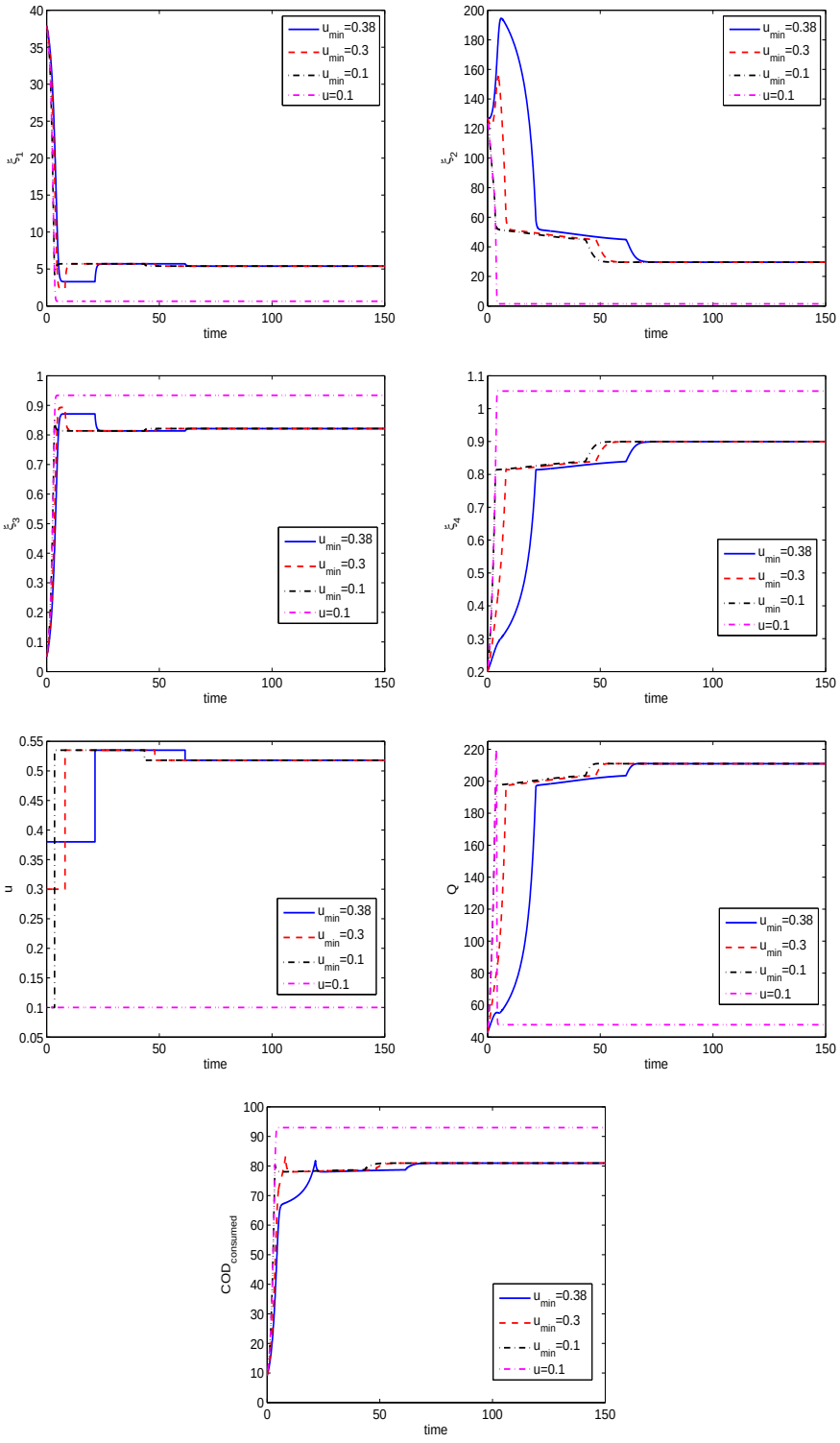

Figure 5: The time evolution of the substrate concentrations ξ_1 and ξ_2, the bacteria concentration ξ_3 and ξ_4, the control law u, the biogas outflow rate Q and the consumed COD (%): controlled system (for three values of u_{min}) and uncontrolled system (low constant dilution rate)

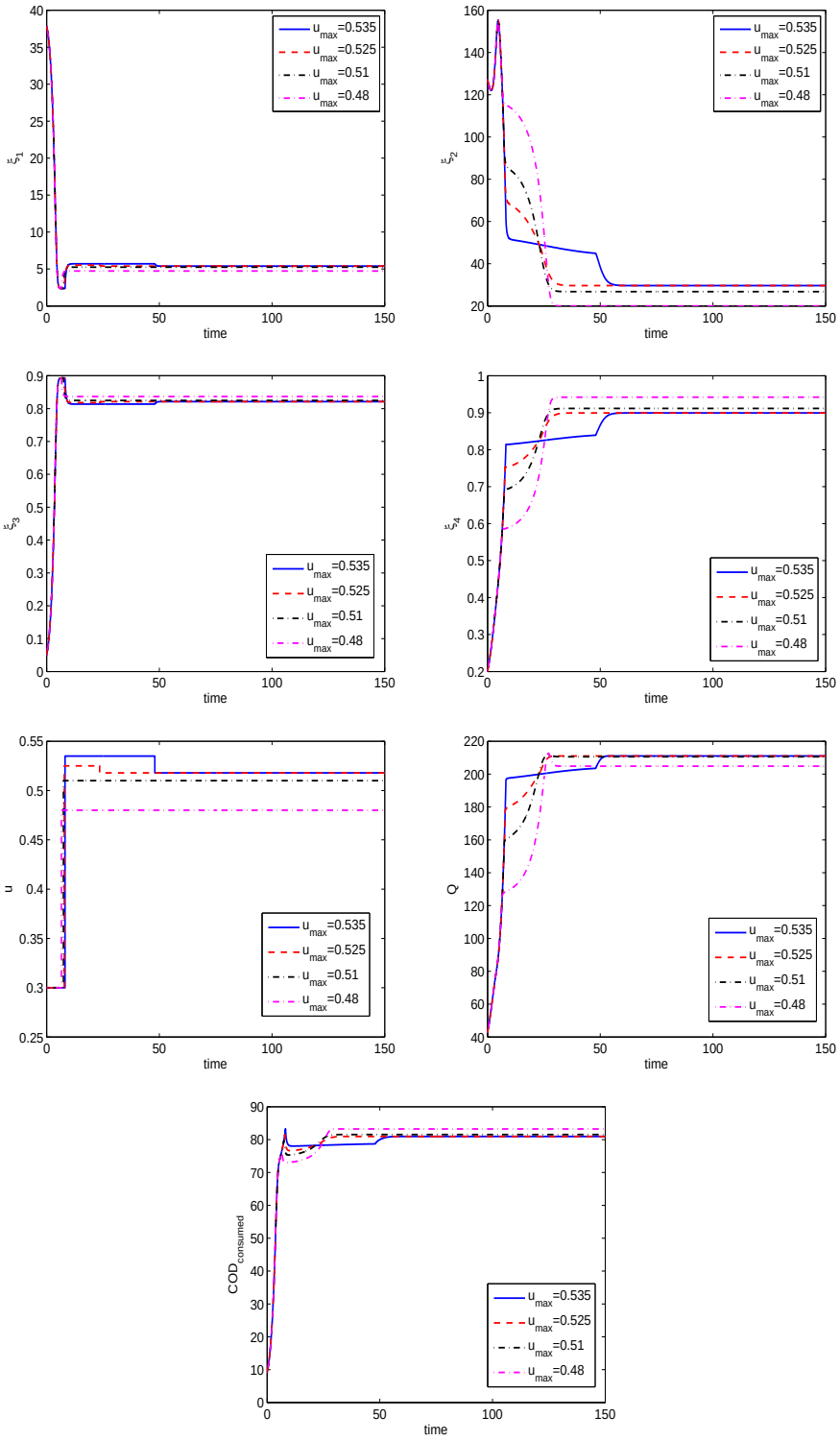

Figure 6: The time evolution of the substrate concentrations ξ_1 and ξ_2, the bacteria concentration ξ_3 and ξ_4, the control law u and the biogas outflow rate Q and the consumed COD (%): controlled case (for four values of u_{max})

where it was assumed that ξ_{in_2} is mainly acetic acid. The COD leaving the reactor is given by the total organic matter in the effluent. Note that organic matter is found also in the biomass (the reactor is operated in continuous mode), hence:

$$COD_{out}(g/l) = \xi_1 + 0.6\xi_2 + 1.42\xi_3 + 1.42\xi_4 \tag{45}$$

The COD consumption is calculated as

$$COD_{consumed}(\%) = \frac{COD_{in} - COD_{out}}{COD_{in}} \cdot 100 \tag{46}$$

which evaluates to 80.96% in the optimal setpoint. Fig. 5 shows that COD consumption rapidly increases to more than 60% and continues to increase further until it reaches the value corresponding to the optimal setpoint. Thus, a high quality of the effluent is achieved together with maximum methane production.

Fig. 5 illustrates also the system states, biogas outflow and COD consumption corresponding to the operation of the system with low, constant dilution rate, a common practice for starting-up the bioreactor. It is worth noticing that, although the COD consumption settles at a high rate (around 92.96%), the biogas outflow quite rapidly drops to a low level (compared to the one achieved in the optimal steady state) and, in order to limit the loss, a controller must be introduced in the loop.

Fig. 6 presents the system states, control laws, biogas outflows and COD consumption rates for four values of u_{max}: 0.535, 0.525, 0.51, 0.48 day^{-1}. The first two cases correspond to $u_s < u_{max}$, the last two correspond to $u_s > u_{max}$. When it is technologically not possible to select u_{max} higher than the solution of the steady state optimization u_s, then the optimal setpoint cannot be reached. Thus, $t_f = \infty$. In those cases, the dilution rate only changes from u_{min} to u_{max} and the system settles down in the equilibrium point $\hat{x}_E^{u_{max}}$. The loss in the steady state productivity is:

$$Q_{loss} = Q(\hat{x}_s) - Q(\hat{x}_E^{u_{max}}) = q(u_s \cdot \hat{x}_{4,s} - u_{max} \cdot \hat{x}_{4,E}^{u_{max}}) \tag{47}$$

and a slight increase of COD consumption may be noticed. The transient times and the loss in the steady state productivity are given in Table 4 for several values of the maximum dilution rate u_{max}.

5 Conclusion

An optimizing start-up strategy for a bio-methanator has been presented in this paper. The procedure consists of steady state optimization as well as transient optimization. A simple suboptimal control law has been derived, which exploits the

Table 4: The transient period and the loss in the steady state productivity for several choices of u_{max}

u_{max}	t_f	Q_{loss}
0.535	47.99	0
0.525	23.52	0
0.51	∞	0.42
0.48	∞	6.16

system characteristics and uses the information provided by Pontryagin's maximum principle: the system must be operated with the minimum dilution rate u_{min} until the switching surface is reached, then it must be operated with the maximum dilution rate u_{max} until it enters a small neighbourhood of the optimal setpoint where the dilution rate is changed to u_s. The proposed control strategy enlarges considerably the region of attraction of the optimal equilibrium point, which for some values of the minimum dilution rate u_{min} becomes quasi-globally asymptotically stable. Thus, if initially both bacteria type are present in the reactor, then the optimal steady state will be reached. Fast and high efficiency of the treatment is achieved, which is particularly remarkable for anaerobic processes operated in continuous mode.

To avoid the tremendous simulation work required for the selection of an appropriate switching surface, one of the system stability boundaries is used to switch the dilution rate from u_{min} to u_{max}. This boundary can be accurately estimated using algorithms that involve a low computational effort. Investigations related to finding better switching surfaces (from the optimality perspective of the cost index (28)) is beyond the scope of this paper: here the emphasis is on the fact that during start-up, high production of biogas must not be trade-off to treatment efficiency, both of them can be reasonably accomplished using a simple switching strategy such as the one presented here.

Without any further investigation, the proposed technique may be applied to any anaerobic digestion system, taking place in a bioreactor operated in continuous mode and described by a two-population model, in which the acidogenesis and methanogenesis are respectively characterized by Monod and Haldane kinetics. The results presented here (the occurrence of multiple equilibrium points, their stability, the existence and the characterization of stability boundaries, the optimal control problem) are generic, they do not depend on the parameter values. If other types of kinetics are considered the switching strategy can still be applied, provided that a preliminary analysis is performed to have the knowledge on the phase portrait structure (the authors have successfully applied this control

strategy to an anaerobic digestion model considering hydrolysis and methanogenesis, where hydrolysis is described by Contois kinetics with inhibition caused by volatile fatty acids). Additionally, to evaluate whether the switching strategy is a good approximation of the optimal one, investigations to establish the (non-)existence of singular intervals in the structure of the optimal control law are needed. This has been done in this paper using explicitly the mathematical expressions of the growth functions.

The robustness evaluation of the proposed strategy with respect to kinetic parameters uncertainty, as well as the extension of the procedure for variable influent concentrations are currently investigated.

6 Appendix

If (t_1, t_2) is a singular interval, then by (42) and (39)

$$s_1(x,p) \equiv 0 \tag{48}$$
$$s_2(x,p) \equiv 0 \tag{49}$$
$$\dot{s_1}(x,p) \equiv 0 \tag{50}$$

From (38) and (49) if follows that for $t_1 < t < t_2$

$$(q - p_4)x_4 = p_3 x_3 \frac{\mu_1(\xi_1)}{\mu_2(\xi_2)} \tag{51}$$
$$x_4 = \frac{p_3 x_3}{(q - p_4)} \frac{\mu_1(\xi_1)}{\mu_2(\xi_2)} \tag{52}$$

while from (37) and (50) it follows that

$$\begin{aligned} \dot{s_1}(x,p) = &-p_3 x_3 \mu_1'(\xi_1)(\xi_{in_1} - \xi_1) + \\ &(q - p_4)x_4 \mu_2'(\xi_2)(\xi_{in_2} - \xi_2) - q\mu_2(\xi_2)x_4 \equiv 0 \end{aligned} \tag{53}$$

Using (51) and (52) in (53) leads to

$$\begin{aligned} p_3 x_3 \cdot \Bigg[&-\mu_1'(\xi_1)(\xi_{in_1} - \xi_1) + \frac{\mu_1(\xi_1)}{\mu_2(\xi_2)} \mu_2'(\xi_2)(\xi_{in_2} - \xi_2) - \\ &\frac{q}{q - p_4} \mu_1(\xi_1) \Bigg] \equiv 0 \end{aligned} \tag{54}$$

Two possibilities result from (54):

Case 1

$$p_3 x_3 \equiv 0 \tag{55}$$

In this case, $p_3 \equiv 0$ as $x_3 \neq 0$. Then, $\dot{p}_3 \equiv 0$, which becomes using the costates equation (33)

$$(q - p_4) x_4 \mu_2'(\xi_2) c \equiv 0 \tag{56}$$

As $x_4 \neq 0$, it follows that

$$p_4 = q \tag{57}$$

and consequently $\dot{p}_4 = 0$ since q is constant. However, using (57) in the costates equation (34) leads to

$$\dot{p}_4 = p_4 u \tag{58}$$

which is in contradiction with $\dot{p}_4 = 0$. Hence, (55) does not hold for $t_1 < t < t_2$.

Case 2

$$\mu_1'(\xi_1)(\xi_{in_1} - \xi_1) - \frac{\mu_1(\xi_1)}{\mu_2(\xi_2)} \mu_2'(\xi_2)(\xi_{in_2} - \xi_2) + \frac{q}{q - p_4} \mu_1(\xi_1) \equiv 0 \tag{59}$$

In this case, $\mu_1'(\xi_1)$ and $\mu_2'(\xi_2)$ are calculated from (8) and (9) as

$$\mu_1'(\xi_1) = \mu_{m_1} \frac{K_{s_1}}{(K_{s_1} + \xi_1)^2} \tag{60}$$

$$\mu_2'(\xi_2) = \mu_{m_2} \frac{K_{s_2} - \frac{\xi_2^2}{K_{i_2}}}{\left(K_{s_2} + \xi_2 + \frac{\xi_2^2}{K_{i_2}}\right)^2} \tag{61}$$

Using (60) and (61) in (59) leads to

$$K_{s_1} \xi_2 \left(K_{s_2} + \xi_2 + \frac{\xi_2^2}{K_{i_2}}\right)(\xi_{in_1} - \xi_1) - \xi_1 (K_{s_1} + \xi_1) \left(K_{s_2} - \frac{\xi_2^2}{K_{i_2}}\right)(\xi_{in_2} - \xi_2) + \frac{q}{q - p_4} \xi_1 (K_{s_1} + \xi_1) \xi_2 \left(K_{s_2} + \xi_2 + \frac{\xi_2^2}{K_{i_2}}\right) \equiv 0 \tag{62}$$

Relationship (62) is a quadratic equation in ξ_1 with the solutions

$$\xi_{1_1} = f_1(\xi_2, p_4) \tag{63}$$
$$\xi_{1_2} = f_2(\xi_2, p_4) \tag{64}$$

Since $\xi_1 = x_1 - ax_3$, it follows that for $t_1 < t < t_2$

$$x_{1_1} = f_1(\xi_2, p_4) + ax_3 \tag{65}$$
$$x_{1_2} = f_2(\xi_2, p_4) + ax_3 \tag{66}$$

which is in contradiction with the fact that x_1 is the solution of $\dot{x}_1 = u(w_1 - x_1)$ for all $t \geq 0$. Hence (59) does not hold.

Thus, it is concluded that singular intervals cannot occur.

References

[1] L. Mailleret, O. Bernard and J. P. Steyer, Robust regulation of anaerobic digestion processes, Water Sci. Technol., 48, 87–94 (2003)

[2] R. Antonelli, J. Harmand, J. P. Steyer and A. Astolfi, Set-point regulation of an anaerobic digestion process with bounded output feedback, IEEE T. Contr. Syst. T., 11, 495–504 (2003)

[3] H.O. Méndez-Acosta, B. Palacios-Ruiz, V. Alcaraz-González, V. González-Álvarez and J. P. García-Sandoval, A robust control scheme to improve the stability of anaerobic digestion processes, J. Process Control, 20, 375–383 (2010)

[4] L. Mailleret, O. Bernard and J. P. Steyer, Nonlinear adaptive control for bioreactors with unknown kinetics, Autom., 40, 1379–1385 (2004)

[5] N.I. Marcos, M. Guay, D. Dochain and T. Zhang, Adaptive extremum-seeking control of a continuous stirred tank bioreactor with Haldane's kinetics, J. Process Control, 14, 317–328 (2004)

[6] N. Dimitrova and M. Krastanov, Nonlinear stabilizing control of an uncertain bioprocess model, Int. J. Appl. Math. Comput. Sci., 19, 441–454 (2009)

[7] J.P. Steyer, O. Bernard, D. Batstone and I. Angelidaki, Lessons learnt from 15 years of ICA in anaerobic digesters, Water Sci. Technol., 53, 25–33 (2006)

[8] S. Shen, G.C. Premier, A. Guwy and R. Dinsdale, Bifurcation and stability analysis of an anaerobic digestion model, Nonlinear Dyn., 48, 391–408 (2007)

[9] J. Hess and O. Bernard, Design and study of a risk management criterion for an unstable anaerobic wastewater treatment process, J. Process Control, 18, 71–79 (2008)

[10] J. Hess and O. Bernard, Advanced dynamical risk analysis for monitoring anaerobic digestion process, Biotechnol. Prog., 25, 643–653 (2009)

[11] B. Benyahia, T. Sari, B. Cherki and J. Harmand, Equilibria of an anaerobic wastewater treatment process and their stability, in "Proceedings of the 11th International Symposium on Computer Applications in Biotechnology", Leuven, Belgium, 371–376 (2010)

[12] F. Logist, I.Y. Smets and J.F. Van Impe, Derivation of generic optimal reference temperature profiles for steady-state exothermic jacketed tubular reactors, J. Process Control, 18, 92–104 (2008)

[13] F. Logist, P.M. Van Erdeghem and J.F. Van Impe, Efficient deterministic multiple objective optimal control of (bio)chemical processes, Chem. Eng. Sci., 64, 2527–2538 (2009)

[14] O. Bernard, Z. Hadj-Sadok, D. Dochain, A. Genovesi and J.P. Steyer, Dynamical model development and parameter identification for an anaerobic wastewater treatment process, Biotechnol. Bioeng., 75, 424–438 (2001)

[15] G. Bastin and D. Dochain, On-line Estimation and Adaptive Control of Bioreactors. Elsevier, Amsterdam (1990)

[16] M. Sbarciog, M. Loccufier and E. Noldus, Determination of appropriate operating strategies for anaerobic digestion systems, Biochem. Eng. J, 51, 180–188 (2010)

[17] M. Sbarciog, M. Loccufier and E. Noldus, The computation of stability boundaries in state space for a class of biochemical engineering systems, J. Comput. Appl. Math., 215, 557–567 (2008)

[18] C. García-Diéguez, F. Molina, E. Roca, Multi-objective cascade controller for an anaerobic digester, Proc. Biochem., 46, 900–909 (2011)

[19] J.R. Banga, E. Balsa-Canto, C. G. Moles and A. A. Alonso, Dynamic optimization of bioprocesses: Efficient and robust numerical strategies, J Biotechnol, 117, 407–419 (2005)

[20] M. Sbarciog, M. Loccufier and E. Noldus, Optimality and stability in a class of bang-bang controlled biochemical reaction systems, Int. J. Control, 81, 836–850 (2008)

[21] M. Sbarciog, M. Loccufier and E. Noldus, Anticipating operational and wash out conditions in biotechnological reactors, AIP Conf. Proc., 839, 618–629 (2006)

[22] M. Sbarciog, M. Loccufier and E. Noldus, The estimation of stability boundaries for an anaerobic digestion system, in "Proceedings of the 11th International Symposium on Computer Applications in Biotechnology", Leuven, Belgium, 359–364 (2010)

[23] P. Masci, O. Bernard, F. Grognard, E. Latrille, J. B. Sorba and J. P. Steyer, Driving competition in a complex ecosystem: application to anaerobic digestion, in "Proceedings of the 10th ECC Conference", Budapest, Hungary, (2009)

[24] N.F. Gray, Water Technology: An Introduction for Environmental Scientists and Engineers. Elsevier Science & Technology Books, Amsterdam (2005)